J Membrane Biol (2011) 239:5–14
DOI 10.1007/s00232-010-9321-y

ORIGINAL ARTICLES

Membrane Partitioning: "Classical" and "Nonclassical" Hydrophobic Effects

Mónica Fernández-Vidal · Stephen H. White · Alexey S. Ladokhin

Received: 15 August 2010 / Accepted: 5 November 2010 / Published online: 8 December 2010

Abstract The free energy of transfer of nonpolar solutes from water to lipid bilayers is often dominated by a large negative enthalpy rather than the large positive entropy expected from the hydrophobic effect. This common observation has led to the idea that membrane partitioning is driven by the "nonclassical" hydrophobic effect. We examined this phenomenon by characterizing the partitioning of the well-studied peptide melittin using isothermal titration calorimetry (ITC) and circular dichroism (CD). We studied the temperature dependence of the entropic ($-T\Delta S$) and enthalpic (ΔH) components of free energy (ΔG) of partitioning of melittin into lipid membranes made of various mixtures of zwitterionic and anionic lipids. We found significant variations of the entropic and enthalpic components with temperature, lipid composition and vesicle size but only small changes in ΔG (entropy–enthalpy compensation). The heat capacity associated with partitioning had a large negative value of about -0.5 kcal mol^{-1} K^{-1}. This hallmark of the hydrophobic effect was found to be independent of lipid composition. The measured heat capacity values were used to calculate the hydrophobic-effect free energy $\Delta G_{h\Phi}$, which we found to dominate melittin partitioning regardless of lipid composition. In the case of anionic membranes, additional free energy comes from coulombic attraction, which is characterized by a small effective peptide charge due to the lack of additivity of hydrophobic and electrostatic interactions in membrane interfaces [Ladokhin and White J Mol Biol 309:543–552, 2001]. Our results suggest that there is no need for a special effect—the nonclassical hydrophobic effect—to describe partitioning into lipid bilayers.

Keywords Heat capacity · Hydrophobic effect · "Nonclassical" hydrophobic effect

M. Fernández-Vidal · S. H. White (✉)
Department of Physiology and Biophysics and the Center for Biomembrane Systems, University of California, Irvine, CA 92697-4560, USA
e-mail: stephen.white@uci.edu

A. S. Ladokhin (✉)
Department of Biochemistry and Molecular Biology, University of Kansas Medical Center, Kansas City, KS 66160-7421, USA
e-mail: aladokhin@kumc.edu

Present Address:
M. Fernández-Vidal
Department of Peptide and Protein Chemistry, IIQAB-CSIC, 08034 Barcelona, Spain

Introduction

Understanding biochemical processes such as membrane protein folding, protein-mediated membrane fusion, transmembrane signal transduction and protein translocation across membranes requires an understanding of the energetics of protein insertion into and stability within lipid bilayers. The major driving force for partitioning solutes into nonpolar phases is universally assumed to be the hydrophobic effect, which arises from the tendency of nonpolar molecules to avoid contact with water. This makes the hydrocarbon core of lipid bilayers a favorable environment for nonpolar solutes (Tanford 1980). The hydrophobic effect is generally considered to arise from the release of ordered water molecules around the solute's nonpolar surface. Partitioning into lipid bilayers is much more complicated than bulk-phase partitioning, owing primarily to the anisotropic and heterogeneous nature of bilayers (Huang and Charlton 1972; Schwarz and Beschiaschvili 1989; Seelig and Ganz 1991; Simon et al. 1977;

White 1976; Wiener and White 1992; Wimley and White 1993). This becomes apparent from the relative contributions of enthalpy and entropy to transfer free energies. For bulk phases at room temperature, entropy arising from the hydrophobic effect is dominant, whereas for bilayers enthalpy is often dominant (Huang and Charlton 1972; Seelig and Ganz 1991; Tanford 1980). This enthalpy-driven partitioning, referred to as the "nonclassical" hydrophobic effect (Huang and Charlton 1972; Seelig and Ganz 1991), appears to be a unique feature of solute–bilayer interactions. The suggestion has even been made that "classical" hydrophobic partitioning may not be operative in some, if not all, bilayers (Seelig and Ganz 1991). However, the characterization of complex partitioning processes in lipid bilayers in terms of entropy and enthalpy alone can be misleading (Dill 1990; Murphy et al. 1990; Wimley and White 1993). In considering hydrophobic partitioning, it is important to realize that the true hallmark of the hydrophobic effect is the large negative heat capacity associated with the dehydration of nonpolar surfaces (Baldwin 1986). Following the approach of Wimley and White (1993) for a series of indole compounds, we show here that consideration of the heat capacity of melittin partitioning into bilayers eliminates the need to invoke the nonclassical hydrophobic-effect idea.

Using isothermal titration calorimetry and circular dichroism (CD) spectroscopy, we reexamined the bilayer partitioning of the well-studied peptide melittin, which is included in the group of peptides whose partitioning is supposedly driven by the nonclassical hydrophobic effect (Seelig 1997). We determined the temperature dependence of the entropic ($-T\Delta S$) and enthalpic (ΔH) components of the partitioning free energy (ΔG) of melittin into lipid membranes made of various mixtures of zwitterionic and anionic lipids. Our results show that the hydrophobic effect is the main driving force for partitioning, regardless of the relative contributions of entropy and enthalpy.

Materials and Methods

Materials

Lipids were obtained from Avanti Polar Lipids (Alabaster, AL), and melittin (sequencing grade) was from Sigma (St. Louis, MO). The buffer, a 10 mM potassium phosphate solution (pH 7.0), was used to reduce UV absorbance in CD experiments.

Preparation of Vesicles

A defined amount of lipid in chloroform was first dried under nitrogen and then overnight under high vacuum. Typically, 1–2 ml of buffer (10 mM potassium phosphate solution, pH 7.0) was added to the lipid and the dispersion extensively vortexed. For preparation of small unilamellar vesicles (SUVs), the lipid dispersion was sonicated in an ice-water bath using a titanium tip ultrasonicator until the solution became transparent. Metal debris from the titanium tip was removed by centrifugation (Eppendorf table-top centrifuge, 25 min at 10,000 rev/min). Large unilamellar vesicles (LUVs) of the lipids with an approximate diameter of 0.1 μM were formed by extrusion under nitrogen through Nucleopore (Pleasanton, CA) polycarbonate membranes (10 times through two stacked 0.1-μm filters), using the method of Mayer et al. (1986).

High-Sensitivity Titration Calorimetry

Isothermal titration calorimetry (ITC) was performed using a MicroCal (Norhampton, MA) MC-2 high-sensitivity titration calorimeter. Solutions were degassed under vacuum prior to use. The calorimeter was calibrated electrically. In ITC experiments, the calorimeter cell (1.3 ml) was filled with the suspension of lipid vesicles ($\sim$5 mM), and injections of melittin (10 μL) were made every 4.5 min with a 250-μl Hamilton (Reno, NV) syringe. The concentration of melittin was around 100 μM. Under these conditions, concentrations of lipid greatly exceed those of the peptide during the whole titration experiment, and the injected peptide is completely bound to the membrane surface. Thus, each injection experiment produces the same heat of reaction. Control experiments with injection of buffer into buffer, buffer into lipid and melittin into buffer were performed. Experiments were performed between 25 and 60°C. The heat of dilution was subtracted from the heat determined in the corresponding peptide/lipid binding experiments. Data were acquired using software developed by Microcal.

CD and Absorbance Spectroscopy

CD measurements were performed using a Jasco-720 spectropolarimeter (Japan Spectroscopic, Tokyo, Japan). Normally, 10–30 scans were recorded between 190 and 260 nm, using a 1-mm optical path. Spectra were corrected for background scattering by subtracting a vesicle-only spectrum measured with an appropriate concentration of vesicles in buffer, without the peptide. Temperature was controlled by a Peltier unit. Experiments were performed between 5 and 60°C. UV absorbance was measured with a Cary 3E spectrophotometer (Varian Analytical Instruments, Sugar Land, TX). Molar concentrations were determined using a molar extinction coefficient of $\varepsilon_{280} = 5{,}600\ \mathrm{M}^{-1}\ \mathrm{cm}^{-1}$ for tryptophan. Measured values of ellipticity were converted into ellipticity per amino acid

residue by dividing by the length of the optical path, molar peptide concentration and number of amino acid residues in the peptide. CD and absorbance were measured in the same cuvette in order to minimize errors in determination of molar ellipticity.

The fractional helical content (f_α) of melittin can be estimated using the formula

$$f_\alpha = \Theta - \Theta_{RC}/\Theta_H - \Theta_{RC} \quad (1)$$

where Θ is observed ellipticity and Θ_{RC} and Θ_H are the limiting values for a completely random coil and a completely helical conformation, respectively. Although this formula is simple and well accepted, there is a certain ambiguity in the result due to the uncertainty in prediction of what the actual values for Θ_{RC} and Θ_H should be. Here, we used the formula derived by Luo and Baldwin (1997):

$$\Theta_{RC} = 640 - 40T \quad (2)$$

$$\Theta_H = -42,500 + 125T \quad (3)$$

where T is the experimental temperature. Quantitatively, a melittin molecule, bound to a lipid membrane at 25°C, shows a conformation with ~70% α-helical content corresponding to 18–19 amino acids, which is in good agreement with previous results (Ladokhin and White 1999; Vogel 1981).

Changes of the CD signal depending on the lipid concentration can therefore be used to determine quantitatively the relevant association isotherm, i.e., the amount of associated peptide for lipid as a function of the free aqueous peptide concentration.

Calculated CD Spectra

Calculated CD spectra for melittin bound 100% to LUVs and SUVs were obtained from the spectra for 0 and 5 mM lipid concentrations. The fraction of melittin bound at 5 mM was estimated to be 70% for LUVs and 95% for SUVs, based upon the measured partitioning free energy, ΔG. The contribution of the free peptide was subtracted (30% for LUVs, 5% for SUVs) from the spectra measured in the presence of 5 mM lipid in order to estimate the spectra for 100% binding.

Data Analysis

The free energies of transfer ΔG of melittin were determined from the mole fraction partition coefficient K_X using $\Delta G = -RT\ln K_X$. K_X is the mole fraction partition given by

$$K_X = \frac{[P]_{bil}/[L]}{[P]_{water}/[W]} \quad (4)$$

where $[P]_{bil}$ and $[P]_{water}$ are the bulk molar concentrations of peptide attributable to peptide in the bilayer and water phases, respectively; $[L]$ and $[W]$ are the molar concentrations of lipid and water (55.3 M). Given that $[P]_{total} = [P]_{bil} + [P]_{water}$, one can easily show that

$$f_p = \frac{K_X[L]}{[W] + K_X[L]} \quad (5)$$

where f_p is the fraction of peptide bound. K_X was determined by least-squares fitting of Eq. 5 to plots of f_p against $[L]$ using the Origin 7.0 software package (OriginLab, Northampton, MA).

The fraction of peptide bound was determined by titration measurements using CD measurements, described in detail by White et al. (1998):

$$\Theta_{norm} = 1 + (\Theta_m - 1)\frac{K_X[L]}{[W] + K_X[L]} \quad (6)$$

where Θ_{norm} is the normalized molar ellipticity of the peptide and Θ_m is the increase in the normalized molar ellipticity of the peptide upon binding to in the membrane.

The partition coefficient at 25°C, the van't Hoff enthalpy and the heat capacity change were evaluated according to the van't Hoff relationship (Naghibi et al. 1995):

$$\ln K_{a,T} = \ln K_{a,ref} - \frac{\Delta H_{ref}}{R}\left(\frac{1}{T} - \frac{1}{T_{ref}}\right) + \frac{\Delta C_p}{R}\left[\left(\frac{T_{ref} - T}{T}\right) + \ln\frac{T}{T_{ref}}\right] \quad (7)$$

in which $K_{a,T}$ is the association constant at temperature T, $K_{a,ref}$ and T_{ref} refer to an arbitrary reference temperature near the middle of the range of the data (298 K), ΔH_{ref} is the enthalpy change at T_{ref} and ΔC_p is the change in heat capacity (assumed to be constant over the experimental range of temperature).

All fits of experimental data to equations were performed with Origin 7.0. ITC data were acquired by computer using software developed by Microcal.

Results

CD Experiments

The secondary structure and the free energies of melittin partitioning into LUVs formed from mixtures of 1-palmitoyl-2-oleoyl-*sn*-glycero-3phosphatidylcholine (POPC) and 1-palmitoyl-2-oleoyl-*sn*-glycero-3-phosphoglycerol (POPG) (0%, 10%, 25% and 50%) at different temperatures (5, 15, 25, 40, 50 and 60°C) were determined using CD spectroscopy. Typical titration data obtained by CD are shown in Fig. 1 for melittin partitioning into POPC membranes. Melittin in solution has a random coil structure,

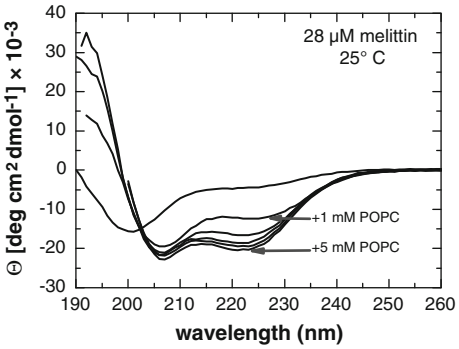

Fig. 1 CD measurements of partitioning-folding coupling of membrane interactions of melittin. Titration with POPC LUVs results in progressive formation of α-helical conformation. The existence of an isodichroic point at 204 nm indicates the existence of only two conformations: unfolded peptide in solution and folded peptide in the membrane. Binding isotherms based on measurements of ellipticity at 222 nm during titration of melittin with vesicles are used to determine helical content (Fig. 2) and the free energy of partitioning (Table 1)

whereas upon partitioning into lipid membranes it adopts a characteristic α-helix ellipticity at 222 nm that progressively increases with increasing lipid concentration. Molar ellipticity at 222 nm was used to determine quantitatively partitioning isotherms, which were fit by least-squares minimization to obtain the maximum ellipticity (Θ_m), mole-fraction partition coefficients (K_X) and consequently ΔG, as described in Materials and Methods. Care was taken to assure that K_X was measured at very low peptide concentrations, typically no higher than one bound peptide molecule per 100 lipid molecules, in order to avoid non-ideal behavior and especially anticooperative binding in the case of charged peptides (Ladokhin et al. 1997; White et al. 1998).

Titration of melittin with vesicles of different diameters (LUVs and SUVs) resulted in clearly different POPC partitioning (data not shown): $\Delta G = -7.2$ kcal mol^{-1} for SUVs and $\Delta G = -6.2$ kcal mol^{-1} for LUVs. This difference cannot be attributed to differences in melittin structure because CD spectra calculated for melittin completely bound to SUVs and LUVs are identical (Ladokhin et al. 2010). Higher partitioning into SUVs has been observed for a number of peptides, including melittin, using other methods of detection (Ladokhin et al. 2000) and is likely related to relief of asymmetric bilayer tension arising from high curvature (see also the discussion of ITC results below).

The free energy of partitioning of positively charged melittin into negatively charged POPC:POPG vesicles increases with POPG concentration, due to electrostatic contributions. The free energy of partitioning of unfolded melittin into the bilayer interface of POPC vesicles has been estimated by various methods to be -6 to -7 kcal mol^{-1} using mole-fraction partition coefficients (Beschiaschvili and Baeuerle 1991; Kuchinka and Seelig 1989; Ladokhin et al. 2000; Ladokhin and White 1999; Schwarz and Beschiaschvili 1989; Vogel 1981). Consistent with these data, we found $\Delta G = -6.2$ (± 0.1) kcal mol^{-1} for POPC and $\Delta G = -7.50$ (± 0.05) kcal mol^{-1} for $POPC_{50}$:$POPG_{50}$, both measured at 25°C. The complete results of free energy measurements using several lipid compositions and for temperatures ranging from 25 to 60°C are presented in Table 1.

The molar ellipticity at 25°C for POPC corresponds to a peptide helical fraction f_α of 0.71, in agreement with previous results (Ladokhin and White 1999; Vogel 1981). For $POPC_{90}$:$POPG_{10}$, $POPC_{75}$:$POPG_{25}$ and $POPC_{50}$:$POPG_{50}$, the values of f_α obtained at 25°C were 0.71, 0.73 and 0.71, respectively. The overall folding of melittin into different lipid mixtures over a range of temperatures is very similar (see Fig. 2); the helicities are maximal near room temperature ($\sim$25°C) and decrease in both directions away from room temperature. For instance, when melittin is titrated with pure POPC at 5°C, the helical fraction of peptide (or the fraction of peptide bound) decreases to $\approx$0.57. In the other direction, the fraction of peptide bound to pure POPC at 60°C is $\approx$0.63. This behavior was very similar for all of the mixtures studied, showing that the peptide binds in similar ways to the different mixtures of lipids. The fraction of peptide bound for $POPC_{50}$:$POPG_{50}$ at 5°C was $\approx$0.57 and that at 60°C was $\approx$0.58. It is also important to note the existence of an isodichroic point at 204 nm for the whole range of temperatures studied (e.g., Fig. 1), indicating that the peptide exists in two states (helical and coiled).

ITC Measurements

The enthalpies of melittin partitioning into SUVs and LUVs composed of various fractions of POPC and POPG were determined with high-sensitivity titration calorimetry by injecting small amounts of peptide solution into lipid suspensions of defined lipid concentration. Figure 3 shows the result of injecting 10-μl aliquots of a 100-μM melittin solution into a suspension of 5 mM POPC and $POPC_{50}$:$POPG_{50}$ LUVs and SUVs at 25°C. Because of the large lipid-to-peptide ratio, the injected peptide was completely bound to the membranes, as indicated by virtually identical heats for consecutive injections. Injections of peptide into buffer and buffer into lipid were done as control, but in these cases the heats of dilution were very small and, thus, neglected.

For POPC LUVs, a positive endothermic enthalpy change was obtained, whereas for POPC SUVs a negative exothermic enthalpy change was found. Before corrections, a value of $\approx$11 kcal mol^{-1} for POPC LUVs was obtained, while for POPC SUVs the value was ≈ -10 kcal mol^{-1}.

Table 1 Thermodynamic parameters for melittin binding to different mixtures of POPC and POPG, ranging 0–50%

POPC (%)	POPG (%)	T (°C)	ΔG (kcal mol^{-1})	ΔH_{cal} (kcal mol^{-1})	$-T\Delta S$ (kcal mol^{-1})	ΔC_p (kcal mol^{-1} K^{-1})[a]	ΔC_p (kcal mol^{-1} K^{-1})[b]
100	0	25	−6.2 (±0.1)	20 (±2)	−26 (±2)		
		40	−6.1 (±0.1)	6.2 (±1.6)	−12.3 (±1.6)	−0.61 (±0.06)	−0.60 (±0.06)
		50	−5.9 (±0.1)	0.3 (±1.4)	−6.2 (±1.4)		
		60	−6.0 (±0.1)	−2.8 (±1.3)	−3.2 (±1.3)		
90	10	25	−6.8 (±0.1)	−0.9 (±1.5)	−5.9 (±1.5)		
		40	−6.95 (±0.06)	−4.7 (±0.9)	−2.25 (±0.9)	−0.34 (±0.03)	−0.47 (±0.05)
		50	−6.7 (±0.1)	−10 (±1)	3.3 (±1)		
		60	−6.77 (±0.05)	−12.5 (±1.1)	5.73 (±1.1)		
75	25	25	−7.12 (±0.03)	−2.7 (±0.6)	−4.42 (±0.6)		
		40	−7.16 (±0.04)	−10.4 (±0.8)	3.24 (±0.8)	−0.56 (±0.04)	−0.35 (±0.05)
		50	−7.28 (±0.08)	−15.6 (±0.4)	8.32 (±0.4)		
		60	−7.34 (±0.08)	−22.4 (±1.1)	15.06 (±1.1)		
50	50	25	−7.50 (±0.05)	−4.7 (±1)	−2.8 (±1)		
		40	−7.82 (±0.04)	−10.9 (±1)	3.08 (±1)	−0.58 (±0.03)	−0.33 (±0.04)
		50	−7.97 (±0.03)	−16.7 (±1.1)	8.73 (±1.1)		
		60	−8.01 (±0.06)	−25 (±1.5)	16.99 (±1.5)		

Data were obtained from ITC experiments and CD experiments. ΔG is the free energy of the partitioning obtained by means of CD spectroscopy; ΔH_{cal} is the calorimetric enthalpy obtained from titration of LUVs with melittin; ΔC_p is the heat capacity change obtained by the slope of the temperature dependence of the enthalpy; $-T\Delta S$ corresponds to the value obtained from the formula $\Delta G = \Delta H - T\Delta S$. Values in parentheses are joint confidence limits

[a] ΔC_p obtained by measurements of enthalpy at different temperatures

[b] ΔC_p obtained by van't Hoff analysis

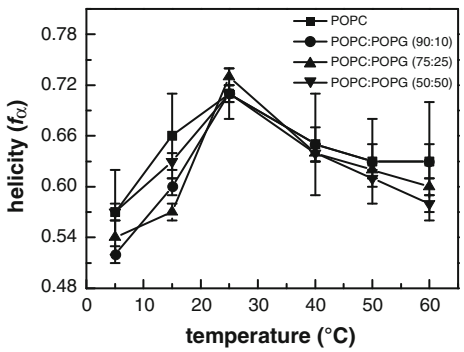

Fig. 2 Temperature dependence of helical content of melittin upon binding to different lipid mixtures. The overall binding of melittin into different lipid mixtures is similar for all temperature ranges

Also, for the mixture $POPC_{50}$:$POPG_{50}$, a more exothermic enthalpy value was found when SUVs were used. For POPC:POPG mixtures, it has been shown that free energies of transfer depend strongly on vesicle curvature so that partition coefficients can be anomalous for the smallest vesicles (Greenhut et al. 1986; Plager and Nelsestuen 1994; Seelig and Ganz 1991). This is an indicator that SUVs are metastable and therefore unsuitable for thermodynamic measurements.

When the lipid headgroup in LUVs is changed from zwitterionic to a mixture of zwitterionic and negatively charged, the membrane association of the peptide became enthalpy-driven (Fig. 3a, c), suggesting that the partitioning mechanisms for charged and uncharged lipids are different. However, as seen in Fig. 2, the helical content of all mixtures was similar over the range of temperatures studied. This suggests that the overall partitioning of melittin into the different mixtures is similar for all the cases.

Thermodynamic Analysis

The temperature dependence of melittin binding to bilayers is presented in Fig. 4a. Partition coefficients increase with temperature up to 25°C and then decrease with further temperature increases to 60°C. Each of the points represents a separate titration of melittin into the lipid membrane at a given temperature. van't Hoff analysis of the partitioning data (Fig. 4a) yields concave-downward curves, as expected for negative changes in heat capacity. At 25°C, $\ln K_X$ increases with the concentration of POPG because the binding is enhanced by increasing concentrations of the negatively charged lipid. The important point is the heat capacity change is negative and very large, which is characteristic of the hydrophobic effect. Moreover, it was very similar for all the mixtures. We obtained a value of approximately -0.5 kcal mol^{-1} K^{-1} for all lipid mixtures.

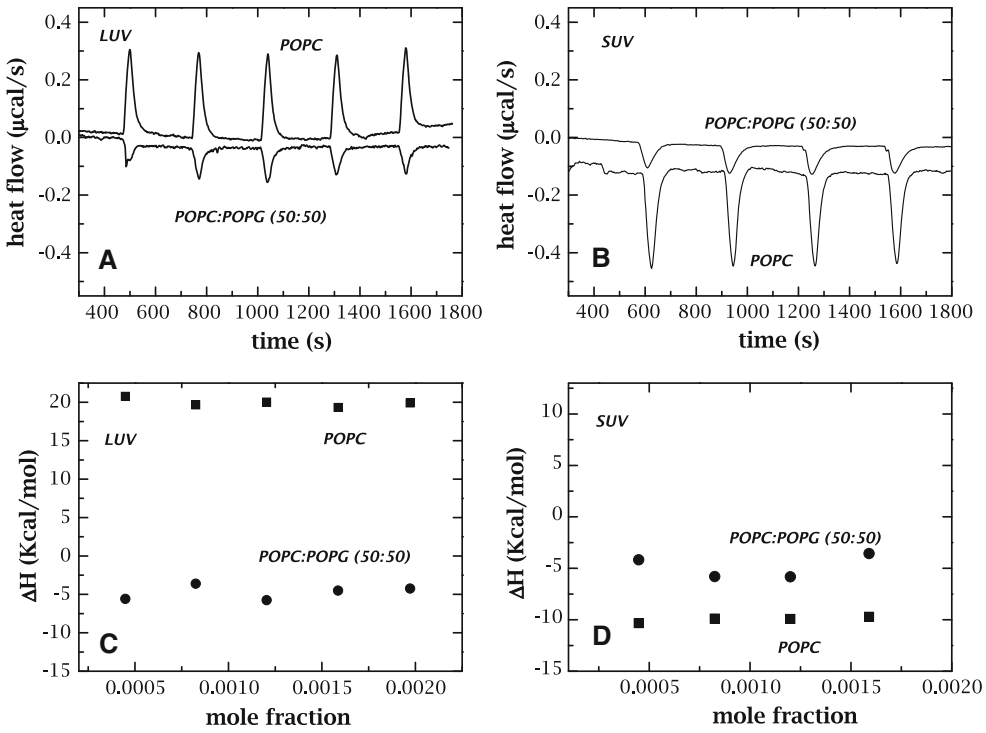

Fig. 3 Titration calorimetry of LUVs (*left panels*) and SUVs (*right panels*) of 5 mM POPC or 3 mM POPC:POPG (50:50) mixture with a 0.1 mM solution of melittin. Titration calorimetry of **a** LUVs and **b** SUVs of POPC and $POPC_{50}$:$POPG_{50}$ with melittin at 25°C. These panels display the heat flow measured after injection of 10-µl aliquots of peptide solution into the calorimeter cell (1.3469 ml) containing a lipid dispersion at a concentration of about 5 mM. Graph shows the calorimetry tracing; upward peaks denote endothermic reactions and downward peaks, exothermic reactions. These graphs yield the heats of reaction as evaluated from the areas underneath the calorimeter tracings (**c** and **d** for LUVs and SUVs, respectively). In these experiments, the lipid concentration greatly exceeds that of the peptide, causing the heat of reaction to be practically identical for all injections. Variations in vesicle size and composition result in dramatic changes in the heat of reaction

Another way to obtain the heat capacity change is by analyzing the temperature dependence of the calorimetric enthalpy, as presented in Fig. 4b. Enthalpy decreases linearly with temperature in all cases and can be fitted to the following equation:

$$\Delta H(T) = \Delta H(T_{\mathrm{m}}) + C_{\mathrm{p}}(T - T_{\mathrm{m}}) \quad (8)$$

The slopes of the curves represent the heat capacity change. In the case of POPC, around 70% of the injected peptide was membrane-bound (deduced from the binding curve obtained by CD measurements). Therefore, the enthalpy of binding to pure POPC has to be scaled to 100% peptide binding; this yields an endothermic value of 20 (±2) kcal mol^{-1}. This correction is not necessary in the case of the mixtures of POPC and POPG because in the presence of the negatively charged lipid complete binding is confirmed by the CD titration data. For every experiment, control titrations of peptide into buffer and lipid into buffer were performed and subtracted when necessary. Table 1 shows the thermodynamic results obtained from ITC experiments. At 25°C, the enthalpy changes ΔH were 20 (±2) kcal mol^{-1} for POPC, −0.9 (±1.5) kcal mol^{-1} for $POPC_{90}$:$POPG_{10}$, −2.7 (±0.6) kcal mol^{-1} for $POPC_{75}$:$POPG_{25}$ and −4.7 (±1) kcal mol^{-1} for $POPC_{50}$:$POPG_{50}$. This shows that increasing the concentration of negatively charged lipid decreases the enthalpy, going from an endothermic enthalpy for POPC to an exothermic value for $POPC_{50}$:$POPG_{50}$. We obtained a very large negative heat capacity change for all lipid mixtures, which is in agreement with the values obtained from the van't Hoff analysis, around −0.5 kcal mol^{-1} K^{-1} (see Table 1).

Figure 5 shows the dependence of the observed free energy, ΔG_{obs}, on surface potential, φ, of melittin, which has an electrical valence of 5–6. ΔG_{obs} varies linearly with φ, computed from Gouy-Chapman theory (see, e.g., Ben-Tal et al. 1996; Ladokhin and White 2001). The slope gives the effective charge of melittin, using the definition $\Delta G_{\mathrm{ES}} = z_{\mathrm{eff}} F \varphi$, where z_{eff} is the effective charge of the peptide and F is the Faraday constant. In this case, a very small effective charge of approximately 1 was obtained (a value of ≈ 2 is found in the literature [Beschiaschvili and Baeuerle 1991]). Therefore, the lipid "senses" a much lower charge than the formal valence of 5–6. The electrostatic attraction is not as high as expected from the net

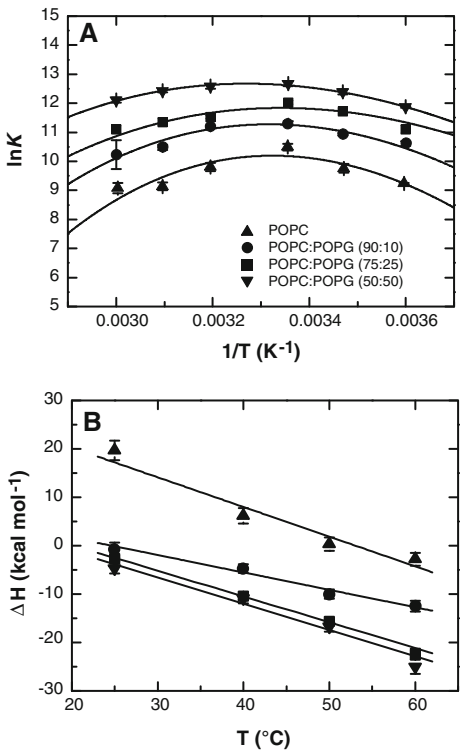

Fig. 4 **a** van't Hoff analysis of the binding of melittin to the lipid membrane obtained by CD titration. van't Hoff plot of $\ln K_a$ vs. $1/T$ for melittin binding different lipid mixtures: POPC, POPC:POPG (90:10) POPC:POPG (75:25) and POPC:POPG (50:50). Each point plotted is from a separate fit to individual binding titration experiments. van't Hoff curves are concave-downward for both directions, indicating a negative change in heat capacity. **b** Temperature dependence of the enthalpy of melittin partitioning into LUVs at different lipid content. In all cases, enthalpy decreases with temperature. The slope of the curves gives the change of heat capacity, which is negative and similar for all cases, about −0.5 kcal/molK

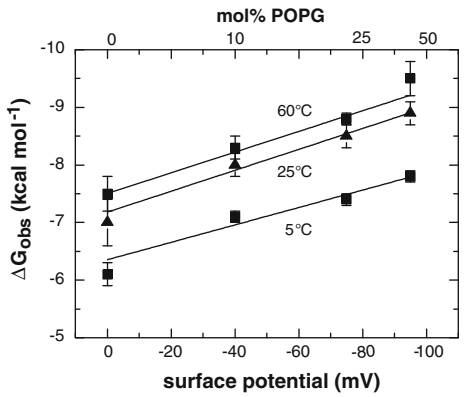

Fig. 5 Experimentally determined free energies of partitioning (ΔG) of melittin into LUVs formed from mixtures of POPC and POPG, ranging 0–50% POPG. Data are plotted against surface potential (φ) computed from Gouy-Chapman theory. The slopes of the curves indicate a small value for the effective charge, consistent with a lack of complete additivity of hydrophobic and electrostatic interactions on membrane interfaces (Ladokhin and White 2001; Posokhov et al. 2007)

charge of melittin. This may explain why Beschiaschvili and Seelig (1990) obtained lower binding constants than we report here. They corrected the free energy of binding to account for the electrostatic component, using the full formal peptide charge in order to arrive at the hydrophobic component. The net effect of this approach is to overcorrect for the electrostatic effect and, consequently, to underestimate the hydrophobic effect. It has been shown that other peptides, e.g., indolicidin variants (Ladokhin and White 2001), ion-channel blockers of the inhibitor cysteine-knot structural family (Posokhov et al. 2007) or polylysine peptides (Ben-Tal et al. 1996), do not obey the electrostatic ideal. Therefore, as Ladokhin and White (2001) found, electrostatic and hydrophobic interactions are not additive in most cases. Indeed, they found a systematic inverse coupling between hydrophobic and electrostatic interactions: Increases in hydrophobicity are accompanied by decreases in the effective charge.

Discussion

The free energy of transfer of nonpolar solutes from water to lipid bilayers is often dominated by a large negative enthalpy rather than the large positive entropy expected from the hydrophobic effect. This common observation has led to the idea that bilayer partitioning requires invocation of the "nonclassical" hydrophobic effect (Seelig and Ganz 1991), which we examined here through measurements of the thermodynamics of melittin partitioning using ITC and CD spectroscopy.

Our thermodynamic analysis of the interaction of melittin with lipid membranes is summarized in Fig. 6. The temperature dependence of the enthalpic (ΔH) and entropic ($-T\Delta S$) contributions to the free energy of the partitioning of melittin into zwitterionic (POPC) and anionic $POPC_{50}$:$POPG_{50}$ mixtures are shown in Fig. 6a. There are significant changes in the entropic and enthalpic components with both temperature and lipid composition. However, some trends can be clearly identified. For example, the slopes of temperature dependence for either enthalpic (solid lines) or entropic (dashed lines) components are essentially the same for the two lipid compositions. The latter similarity, and not the difference in the values at any given temperature, characterizes the essential features of thermodynamic behavior of the system, as revealed though the following analysis of heat capacity.

The contribution of the hydrophobic effect can be distinguished from thermodynamic contributions of the bilayer (bilayer effect) by means of the measured values of heat capacity using the equations (Baldwin 1986; Murphy et al. 1990; Wimley and White 1993)

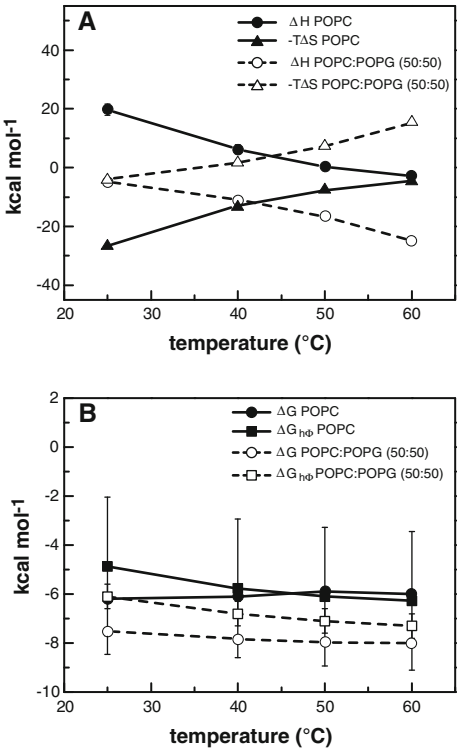

Fig. 6 Summary of the thermodynamic analysis of interaction of melittin with lipid membranes. **a** Temperature dependence of the enthalpic (ΔH) and entropic ($-T\Delta S$) contributions to the free energy of partitioning of melittin into zwitterionic (POPC) and anionic ($POPC_{50}$:$POPG_{50}$) membranes. **b** Temperature dependence of the total free energy (ΔG) and the hydrophobic component of the free energy ($\Delta G_{h\phi}$) for partitioning of melittin into zwitterionic and anionic LUVs. Errors of the free energy ΔG are approximately of the size of the symbols. Errors in the $\Delta G_{h\phi}$ (shown as *bars*) are larger due to the errors in determination of heat capacity (Eq. 7). Despite the significant variation of the entropic and enthalpic components with both temperature and lipid composition (**a**), the total changes in free energy (**b**) are much smaller, due to entropy–enthalpy compensation [note that the scale in (**b**) is almost four times that of (**a**)]. The large negative heat capacity, which corresponds to the slope of the solid lines in (**a**), is independent of lipid composition and a good hallmark of the hydrophobic effect. It can be converted into hydrophobic free energy, $\Delta G_{h\phi}$, which is largely invariable and dominates the total free energy (**b**)

$$\Delta H_{h\phi} = (T - T_h)\Delta C_p \quad (9)$$

$$\Delta S_{h\phi} = \ln(T/T_s)\Delta C_p \quad (10)$$

where T_h and T_s are the values of temperature at which $\Delta H_{h\phi}$ and $\Delta S_{h\phi}$, respectively, have a bulk-phase transfer value of 0. For POPC, T_h and T_s are 326 K and 336 K, respectively; for $POPC_{90}$:$POPG_{10}$, 296 and 316 K; for $POPC_{75}$:$POPG_{25}$, 294 and 306 K; and for $POPC_{50}$:$POPG_{50}$, 292 and 305 K. The contribution of the hydrophobic effect to the free energy of partitioning can be calculated using the formula

$$\Delta G = \Delta C_p(T - T_h) - T\Delta C_p \ln(T/T_s) \quad (11)$$

Using this approach, we calculated a hydrophobic free energy for POPC at 25°C of -4.88 (± 2.83) kcal mol^{-1}. The total free energy for the partitioning of melittin into POPC at that temperature is -6.2 (± 0.1) kcal mol^{-1}, meaning that the contribution of the hydrophobic effect is approximately 79% of the total free energy. $\Delta G_{h\phi} = -6.68$ (± 0.22) kcal mol^{-1} for $POPC_{90}$:$POPG_{10}$ at 25°C. For $POPC_{75}$:$POPG_{25}$ and $POPC_{50}$:$POPG_{50}$ at 25°C, the values are -6.87 (± 0.30) and -7.50 (± 0.52) kcal mol^{-1}, respectively.

Despite the significant variation in the entropic and enthalpic components with both temperature and lipid composition observed (Fig. 6a), the total changes in free energy (Fig. 6b) are much smaller, due to entropy–enthalpy compensation. When the lipid headgroup is changed from zwitterionic to a mixture of zwitterionic and anionic, the membrane association of the peptide became enthalpy-driven. This is a very different result from that of Seelig and Ganz (1991), who concluded that binding enthalpy appeared to be independent of the charge. In their case, however, they performed all the experiments with SUVs. Also, as we show in Fig. 3, the enthalpy changes sign in the experiments performed with POPC LUVs and SUVs. However, the large negative heat capacity is independent of lipid composition (we found a value of approximately -0.5 kcal mol^{-1} K^{-1} for all mixtures), as expected for the hydrophobic effect. The heat capacity values were used to calculate the hydrophobic free energy, which is largely invariable and dominates the total free energy of melittin–bilayer interactions. Additional free energy in the case of anionic membranes comes from coulombic attraction and is characterized by a small effective charge of the peptide, as expected from the lack of additivity of hydrophobic and electrostatic interactions in membrane interfaces (Ladokhin and White 2001; Posokhov et al. 2007). A likely explanation for the nonadditivity is thermodynamic contributions arising from the bilayer's contribution to partitioning (Wimley and White 1993).

We show that the thermodynamics of melittin partitioning depends upon bilayer composition; it is entropy-driven for partitioning into POPC but enthalpy-driven for partitioning into $POPC_{50}$:$POPG_{50}$. Therefore, one might assume that only the binding of melittin to POPC is due to the hydrophobic effect, whereas binding to POPC:POPG is mostly due to electrostatic interactions. However, that assumption would not be correct because the heat capacity change, which is a measure of the hydrophobic effect, is the same for all mixtures, within experimental uncertainties. Therefore, the contribution of the hydrophobic effect is similar for all mixtures, even those containing POPG.

Consequently, the hydrophobic effect must be the main driving force for partitioning melittin into zwitterionic and mixtures of zwitterionic and negatively charged lipids, despite the domination of the enthalpy or entropy components of partitioning free energy in particular cases.

Seelig and Ganz (1991) also found a large value for the heat capacity, characteristic of the hydrophobic effect; but they suggested that the classic hydrophobic effect and the nonclassic hydrophobic membrane partitioning equilibria differ with respect to the temperature dependence of the heat capacity. They did not, however, measure or calculate this temperature dependence. Heat capacity is normally assumed to be constant over the temperature. They also suggested that the observed negative enthalpy values mainly reflect the van der Waals interaction energy between the hydrophobic residues of the solute and the hydrophobic core of the membrane. Wieprecht et al. (2000) calculated the contribution of the nonclassical hydrophobic effect estimated by $\Delta H_{\text{total}} - \Delta H_{\text{helix}}$ and found a value between -5 and -10 kcal mol^{-1}. They concluded that there are three forces driving amphipathic peptides into lipid vesicles: the hydrophobic effect, the coil–helix transition and the nonclassical hydrophobic effect, relating this last to the negative value of the enthalpy. However, is this relationship between enthalpy and the nonclassical hydrophobic effect real? Is the nonclassical effect really a specific effect, or is it the sum of different effects? Wimley and White (1993) showed that the hydrophobic effect is central to bilayer partitioning, but one must consider the relative contribution of bilayer energetics to partitioning (bilayer effect). We suggest that the nonclassical hydrophobic effect is in reality the bilayer effect. The bilayer is not equivalent to a bulk phase. Structurally, it sits in a free energy minimum resulting from the balance of diverse molecular interactions. Because even very low concentrations of bound peptides cause significant changes in bilayer thickness (Hristova et al. 2001; Ludtke et al. 1995), it is reasonable to assume that the presence of bound peptides disturbs this balance, with thermodynamic consequences.

References

Baldwin RL (1986) Temperature dependence of the hydrophobic interaction in protein folding. Proc Natl Acad Sci USA 83: 8069–8072

Ben-Tal N, Honig B, Peitzsch RM, Denisov G, McLaughlin S (1996) Binding of small basic peptides to membranes containing acidic lipids: theoretical models and experimental results. Biophys J 71:561–575

Beschiaschvili G, Baeuerle H-D (1991) Effective charge of melittin upon interaction with POPC vesicles. Biochim Biophys Acta 1068:195–200

Beschiaschvili G, Seelig J (1990) Melittin binding to mixed phosphatidylglycerol phosphatidylcholine membranes. Biochemistry 29: 52–58

Dill KA (1990) The meaning of hydrophobicity. Science 250:297

Greenhut SF, Bourgeois VR, Roseman MA (1986) Distribution of cytochrome b_5 between small and large unilamellar phospholipid vesicles. J Biol Chem 261:3670–3675

Hristova K, Dempsey CE, White SH (2001) Structure, location, and lipid perturbations of melittin at the membrane interface. Biophys J 80:801–811

Huang C-H, Charlton JP (1972) Interactions of phosphatidylcholine vesicles with 2-*p*-toluidinylnaphthalene-6-sulfonate. Biochemistry 11:735–740

Kuchinka E, Seelig J (1989) Interaction of melittin with phosphatidylcholine membranes. Binding isotherm and lipid head-group conformation. Biochemistry 28:4216–4221

Ladokhin AS, White SH (1999) Folding of amphipathic α-helices on membranes: energetics of helix formation by melittin. J Mol Biol 285:1363–1369

Ladokhin AS, White SH (2001) Protein chemistry at membrane interfaces: non-additivity of electrostatic and hydrophobic interactions. J Mol Biol 309:543–552

Ladokhin AS, Selsted ME, White SH (1997) Bilayer interactions of indolicidin, a small antimicrobial peptide rich in tryptophan, proline, and basic amino acids. Biophys J 72:794–805

Ladokhin AS, Jayasinghe S, White SH (2000) How to measure and analyze tryptophan fluorescence in membranes properly, and why bother? Anal Biochem 285:235–245

Ladokhin AS, Fernandez-Vidal M, White SH (2010) CD spectroscopy of peptides and proteins bound to large unilamellar vesicles. J Membr Biol 236:247–253

Ludtke S, He K, Huang H (1995) Membrane thinning caused by magainin 2. Biochemistry 34:16764–16769

Luo PZ, Baldwin RL (1997) Mechanism of helix induction by trifluoroethanol: a framework for extrapolating the helix-forming properties of peptides from trifluoroethanol/water mixtures back to water. Biochemistry 36:8413–8421

Mayer LD, Hope MJ, Cullis PR (1986) Vesicles of variable sizes produced by a rapid extrusion procedure. Biochim Biophys Acta 858:161–168

Murphy KP, Privalov PL, Gill SJ (1990) Common features of protein unfolding and dissolution of hydrophobic compounds. Science 247:559–561

Naghibi H, Tamura A, Sturtevant JM (1995) Significant discrepancies between van't Hoff and calorimetric enthalpies. Proc Natl Acad Sci USA 92:5597–5599

Plager DA, Nelsestuen GL (1994) Direct enthalpy measurements of factor X and prothrombin association with small and large unilamellar vesicles. Biochemistry 33:7005–7013

Posokhov YO, Gottlieb PA, Morales MJ, Sachs F, Ladokhin AS (2007) Is lipid bilayer binding a common property of inhibitor cysteine knot ion-channel blockers? Biophys J 93:L20–L22

Schwarz G, Beschiaschvili G (1989) Thermodynamic and kinetic studies on the association of melittin with a phospholipid bilayer. Biochim Biophys Acta 979:82–90

Seelig J (1997) Titration calorimetry of lipid–peptide interactions. Biochim Biophys Acta 1331:103–116

Seelig J, Ganz P (1991) Nonclassical hydrophobic effect in membrane binding equilibria. Biochemistry 30:9354–9359

Simon SA, Stone WL, Busto-Latorre P (1977) A thermodynamic study of the partition of n-hexane into phosphatidylcholine and phosphatidylcholine-cholesterol bilayers. Biochim Biophys Acta 468:378–388

Tanford C (1980) The hydrophobic effect: formation of micelles and biological membranes. John Wiley & Sons, New York

Vogel H (1981) Incorporation of melittin into phosphatidylcholine bilayers: study of binding and conformational changes. FEBS Lett 134:37–42

White SH (1976) The lipid bilayer as a "solvent" for small hydrophobic molecules. Nature 262:421–422

White SH, Wimley WC, Ladokhin AS, Hristova K (1998) Protein folding in membranes: determining the energetics of peptide–bilayer interactions. Methods Enzymol 295:62–87

Wiener MC, White SH (1992) Structure of a fluid dioleoylphosphatidylcholine bilayer determined by joint refinement of X-ray and neutron diffraction data. III. Complete structure. Biophys J 61:434–447

Wieprecht T, Apostolov O, Seelig J (2000) Binding of the antibacterial peptide magainin 2 amide to small and large unilamellar vesicles. Biophys Chem 85:187–198

Wimley WC, White SH (1993) Membrane partitioning: distinguishing bilayer effects from the hydrophobic effect. Biochemistry 32:6307–6312